Title
Altered carbon turnover processes and microbiomes in soils under long-term extremely high CO2 exposure

Journal
Nature Microbiology, 1(2)

ISSN
2058-5276

Authors
Beulig, Felix
Urich, Tim
Nowak, Martin
et al.

Publication Date
2016

DOI
10.1038/nmicrobiol.2015.25

Peer reviewed

nature microbiology

ARTICLES

PUBLISHED: 27 JANUARY 2016 | ARTICLE NUMBER: 15025 | DOI: 10.1038/NMICROBIOL.2015.25

Altered carbon turnover processes and microbiomes in soils under long-term extremely high CO_2 exposure

Felix Beulig[1], Tim Urich[2,3], Martin Nowak[4], Susan E. Trumbore[4], Gerd Gleixner[4], Gregor D. Gilfillan[5], Kristine E. Fjelland[5] and Kirsten Küsel[1,6]*

There is only limited understanding of the impact of high $p(CO_2)$ on soil biomes. We have studied a floodplain wetland where long-term emanations of temperate volcanic CO_2 (mofettes) are associated with accumulation of carbon from the Earth's mantle. With an integrated approach using isotope geochemistry, soil activity measurements and multi-omics analyses, we demonstrate that high (nearly pure) CO_2 concentrations have strongly affected pathways of carbon production and decomposition and therefore carbon turnover. In particular, a promotion of dark CO_2 fixation significantly increased the input of geogenic carbon in the mofette when compared to a reference wetland soil exposed to normal levels of CO_2. Radiocarbon analysis revealed that high quantities of mofette soil carbon originated from the assimilation of geogenic CO_2 (up to 67%) via plant primary production and subsurface CO_2 fixation. However, the preservation and accumulation of almost undegraded organic material appeared to be facilitated by the permanent exclusion of meso- to macroscopic eukaryotes and associated physical and/or ecological traits rather than an impaired biochemical potential for soil organic matter decomposition. Our study shows how CO_2-induced changes in diversity and functions of the soil community can foster an unusual biogeochemical profile.

Mofettes are low-temperature (<100 °C) fumaroles that emanate almost pure volcanic CO_2 to the atmosphere. These terrestrial venting spots may release >0.5 $tCO_2\ d^{-1}$, leading to consistently high CO_2 soil gas-phase concentrations (>90 vol%)[1], which might be similar to the Earth's atmosphere during the time when photosynthesis evolved[2–4]. The direct and indirect effects of extremely high CO_2 levels on soil biota are poorly studied, but an improved understanding might be important for evaluating the environmental consequences of CO_2 leakages after underground injection or carbon capture and storage (CCS). Because of the often strongly localized venting in close proximity to unaffected reference sites, studies of mofettes can also expand our knowledge of microbial interactions in soil food webs developed under long-term stable hypoxia, in contrast to those sites that experience fluctuations in redox conditions.

Depending on the time and degree of CO_2 exposure, mofettes show distinct geochemical characteristics with features of reductomorphic and acidic soils[5]. For example, lowered pH and redox conditions significantly impact metal(loid) dynamics, thereby potentially affecting soil nutrient availability[6]. Of particular interest is the turnover and storage of carbon (C) in mofettes, as these factors are often associated with the accumulation of soil organic matter (SOM), which appears to increase with depth and $p(CO_2)$ (refs 6,7). It remains unclear whether this accumulation is the result of an overall shift towards increased below-ground C input and/or decreased C mineralization. Intriguingly, a recent study at a floodplain wetland mofette[8] suggested that additional C inputs might result from microbially driven subsurface CO_2 assimilation carried out by anaerobic CO_2-utilizing prokaryotes, for example, acetogens and methanogens. These prokaryotes are also known to be important end members in the complex anaerobic breakdown process for SOM, which is transformed in a catabolic network of consecutive fermentative, syntrophic, acetogenic and/or methanogenic steps, in contrast to oxygen-dependent SOM turnover[9].

The direct or indirect effects of long-term CO_2 emanations could also impair overall soil activity or specific SOM degradation processes, for example, due to anoxic conditions. SOM degradation is generally dependent on the physical and biochemical capabilities of the soil biota[10], and is mediated by a multitude of lignin and carbohydrate metabolizing enzymes underlying biotic and abiotic controls, which we expected to be significantly altered by CO_2 degassings[11]. Assessing the metabolic potential and activity of soil communities as drivers for changes in C cycling has been a focus of ecological research for decades, but largely remains a challenge. With the application of 'meta-omics' approaches in soil ecology[12], it is now possible to put populations, activities and microbial interactions into context with current perceptions of ecosystem functions such as the biogeochemical cycling of C. To date, only a few soil studies have made use of the comprehensive enzyme activity information potential of metatranscriptomics. Prominent examples are investigations of high-Arctic peat[13,14], permafrost soil and thermokarst bog[15]. These studies demonstrated that 'omics' data can correlate with actual rates of key processes and may thus help to elucidate changes in complex soil biochemical networks.

[1]Aquatic Geomicrobiology, Institute of Ecology, Friedrich Schiller University Jena, Dornburger Str. 159, D-07743 Jena, Germany. [2]Division of Archaea Biology and Ecogenomics, Department of Ecogenomics and Systems Biology, University of Vienna, Althanstraße 14, 1090 Vienna, Austria. [3]Bacterial Physiology, Institute for Microbiology, Ernst Moritz Arndt University Greifswald, Friedrich-Ludwig-Jahnstr. 15, 17489 Greifswald, Germany. [4]Max Planck Institute for Biogeochemistry, POB 100164 10, 07701 Jena, Germany. [5]Medical Genetics, Oslo University Hospital and University of Oslo, Kirkeveien 166, 0407 Oslo, Norway. [6]German Centre for Integrative Biodiversity Research (iDiv) Halle-Jena-Leipzig, Deutscher Platz 5e, D-04103 Leipzig, Germany. *e-mail: kirsten.kuesel@uni-jena.de

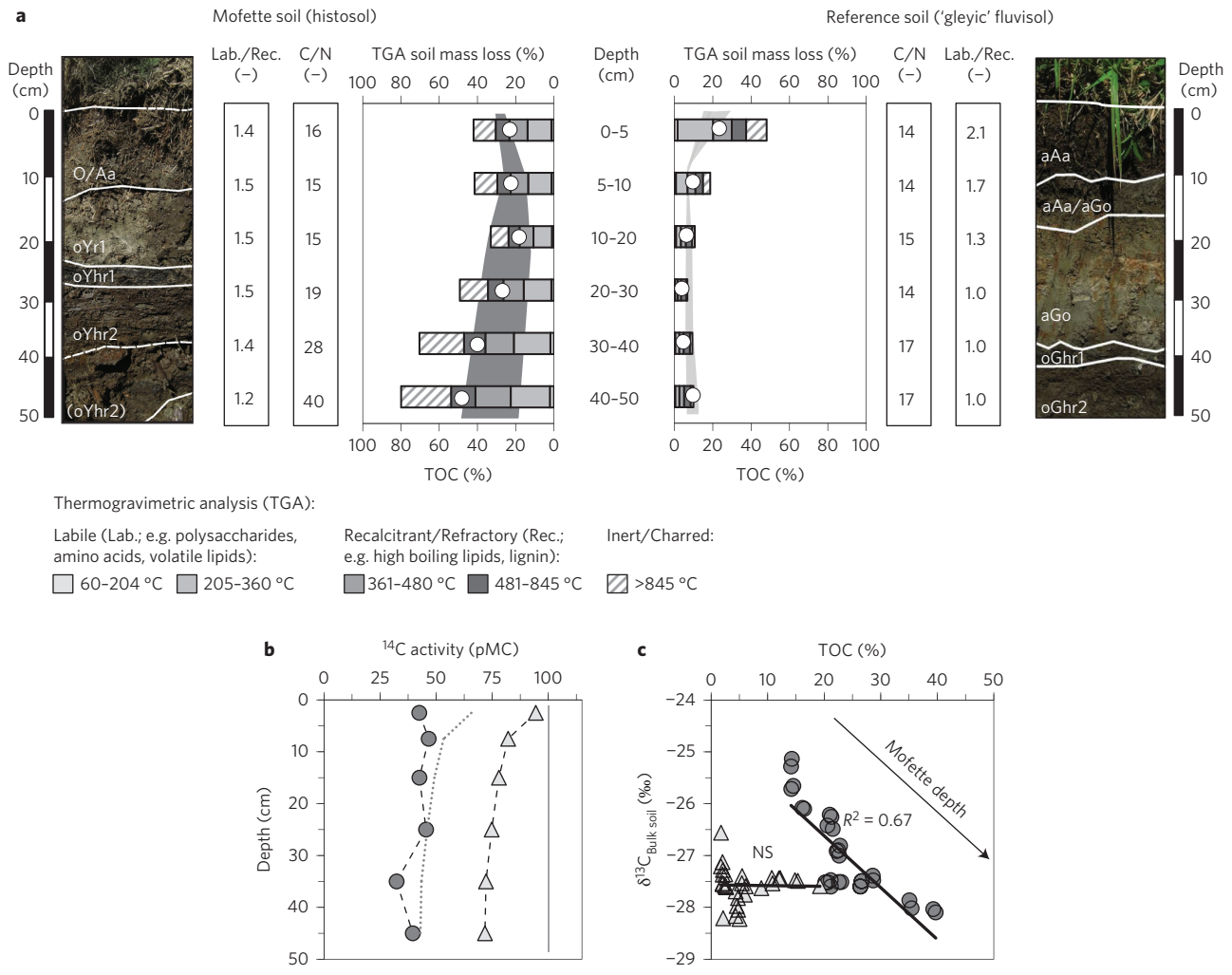

Figure 1 | Bulk soil geochemistry of mofette and reference. a, Soil classification (images are representative of replicate images ($N = 3$) and soil horizon specific images), profiles of relative bulk soil mass loss during TGA, total organic C content (white circles), C/N ratios and ratios of deduced labile and recalcitrant fractions (Lab./Rec.) in mofette and reference soils. Shaded areas depict reported C contents in other mofette and reference soils in this area[6,7]. **b**, Profiles of bulk soil ^{14}C activities in mofette (dark grey circles) and reference (light grey triangles). **c**, Correlation of C content and $\delta^{13}C_{Bulk\ soil}$ (‰ versus VPDB) in mofette (dark grey circles) and reference (light grey triangles). Dotted lines in **b** represent the expected $\Delta^{14}C$ trend based on $\delta^{13}C$ values according to $\Delta^{14}C/\delta^{13}C$ relationships found in plants. Data are shown as mean ± s.d. ($N = 2$; error bars are smaller than symbol size). NS not significant.

We applied a multi-pronged and integrated approach, coupling depth-resolved isotope geochemistry and soil activity analyses to metatranscriptomics and metagenomics, in order to identify processes altering the C turnover in soils under long-term high CO_2 exposure. We show that mofette C mineralization and sequestration may be affected by CO_2-induced changes of diversity and functions across and within trophic levels of the soil food web, which could explain the unusual mofette soil C patterns.

Results and discussion

Accumulation of volcanic C in mofette soils. The studied wetland mofette (50°08′48.4″N, 12°27′04.5″E; Počatky–Plesná fault zone, Czech Republic) was continuously hypoxic at all depths and experienced stable, low redox conditions (Supplementary Fig. 1). It is classified as a histosol with pronounced reductomorphic features (reduced Y horizons; Fig. 1a) due to the influence of upstreaming geogenic gas (>99 vol% CO_2)[1]. In contrast, the floodplain wetland reference soil, classified as 'gleyic' fluvisol, had an oxic/anoxic transition that fluctuated with the water table, accompanied by a decrease in redox potentials at greater depths. Dissolution of emanating CO_2 close to saturation caused only slight pore water acidification ($\Delta pH \approx 0.6$)[6], probably due to buffering by diverse functional groups in the SOM[16].

The total organic carbon (TOC) content in the mofette increased with depth from 22.0 to 47.3 wt% (Fig. 1a), and decreased with depth from 22.9 to 3.7 wt% in the reference. Radiocarbon (^{14}C, expressed as percent Modern C, pMC) decreased with depth in the reference soil (Fig. 1b) from 95.14 pMC (0–5 cm) to 72.31 pMC (40–50 cm), which is typical for soils in the region[17]. In contrast, the mofette bulk soil was consistently more depleted in radiocarbon ($\Delta^{14}C$ activity = 37.63 ± 8.04 pMC) at all depths, providing evidence that a major fraction of the SOM (54–67% 'dead' C) originated from the biotic assimilation of ^{14}C-free volcanic CO_2. The absence of a strong decrease in ^{14}C with depth, as observed in the reference soil profile, can indicate that volcanic-sourced CO_2 is being fixed even at the surface. This was confirmed by radiocarbon analysis demonstrating low ^{14}C contents of 22.31 pMC for the mofette litter and 19.38 pMC for plants growing at the mofette. Stable C isotopes in the bulk mofette soil were enriched in ^{13}C compared with the reference ($\Delta\delta^{13}C$ up to +2.4‰), which is consistent with the use of a 'heavier' geogenic CO_2 source than atmospheric CO_2

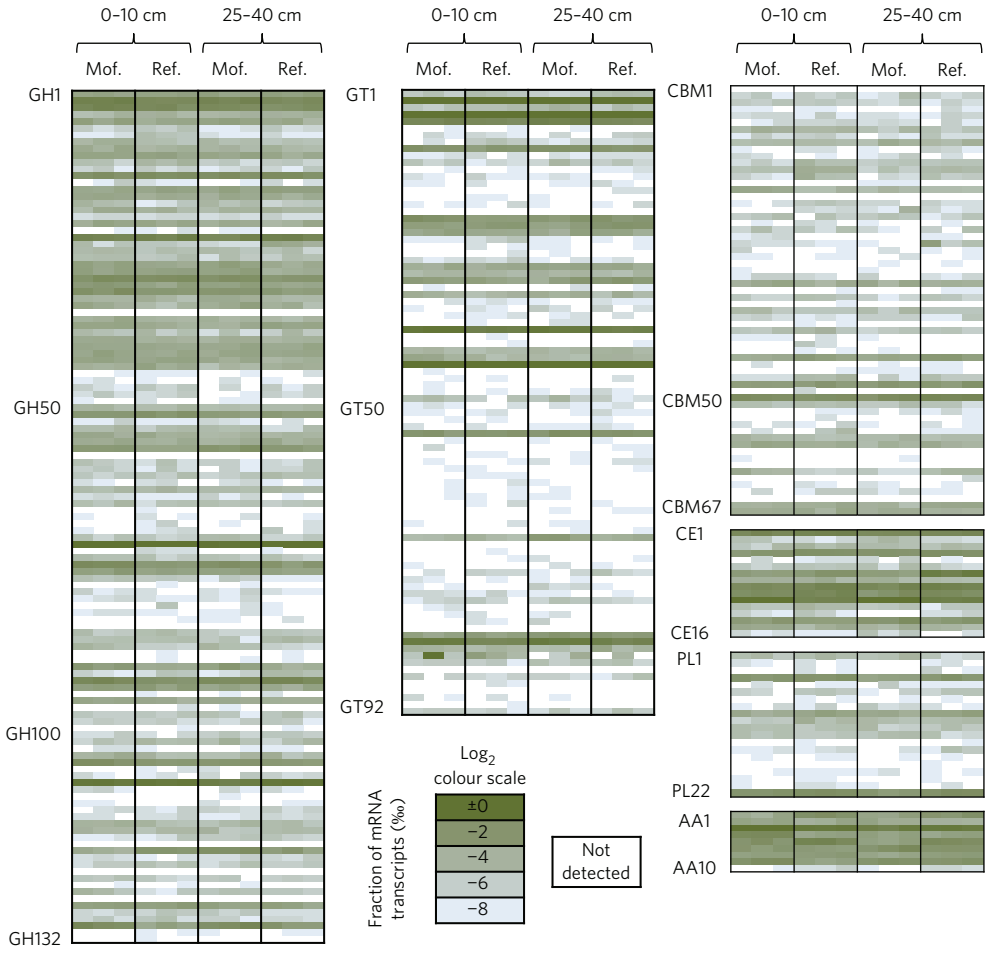

Figure 2 | Frequency profiles of transcripts with annotations of CAZY classes in mofette (Mof.) and reference (Ref.) metatranscriptomes. CAZY classes are presented as glycoside hydrolases (GH), glycoside transferases (GT), auxiliary activities (AA), carbohydrate binding (CBM), carbohydrate esterases (CE) and polysaccharide lyases (PL) in mofette (Mof.) and reference (Ref.) metatranscriptomes. Each sample column contains the results of single replicates ($N = 3$) next to each other.

($\Delta\delta^{13}C \approx +6‰$)[1]. The decreasing $\delta^{13}C$ with depth (Fig. 1c) negatively correlated with the C content in the mofette, either indicating a change in the SOM composition towards ^{13}C-depleted compounds, such as lignins, lipids and their degradation products[18,19], and/or the influence of processes with high C isotope fractionation, for example, methanogenesis or acetogenesis[8,20,21].

In both soils, the particle size of the C fraction below the litter layer was small (<0.05 mm) and suggested at least partially well decomposed organic material. However, pieces of intact plant structures were also found during visual inspection along the mofette soil profile. The C/N ratios in the mofette increased from 16 near the surface to 40 at depth, but remained fairly stable with depth in the reference (15 ± 2). Thermogravimetric analysis (TGA, Fig. 1a) revealed opposing trends in the quantities of thermal labile (for example, polysaccharides), recalcitrant/refractory (for example, lipids) and inert/charred compounds in the soils[22]. Substantial fractions of labile compounds were present throughout the mofette, and while the ratio of labile to recalcitrant fractions was fairly stable at 1.4 ± 0.1 in the mofette, it decreased from 2.1 (0–5 cm) to 1.0 (>20 cm) in the reference. Coupled with the contrasting ^{14}C, $\delta^{13}C$ and C/N patterns, this indicated efficient mineralization in the reference soil, whereas in the mofette less degraded and old organic matter (that is, geogenic C fixed by plants and/or microorganisms) was preserved. As low pH and redox potential over longer timescales led to metal(loid) desorption from and dissolution of major mineral phases[6,8], short-range-order minerals (for example, ferrihydrite) were unlikely to account for C stabilization[23].

Genetic and transcriptional blueprint for SOM decomposition. We investigated mofette and reference soils with metatranscriptomics and metagenomics (Supplementary Tables 1 and 2) at shallow depths (0–10 cm) and below the water table (25–40 cm), with a specific focus on the biochemical potential for SOM degradation. Soil (exo-)enzyme systems are strongly controlled by biotic and abiotic factors[11] and thus are thought to be sensitive to changes in CO_2 levels, geochemistry and substrate (that is, SOM) quantity and composition in the mofette. Despite differences in these parameters in the mofette and reference soils, very similar frequency profiles of individual CAZY (Carbohydrate-Active enZYmes database) classes in all samples (Fig. 2) suggested that the regulation of carbohydrate-metabolizing enzyme synthesis and distribution was largely unaffected by the effects of extreme CO_2 degassing. Eukaryota, especially fungi, are often considered to play a more important role in fresh litter degradation than bacteria[24]. Although CAZY transcripts of eukaryotic origin were abundant in 0–10 cm reference samples (up to 7% of taxonomically annotated CAZY transcripts; Supplementary Table. 3), decomposition processes in both mofette and reference appeared to be mainly mediated by enzymes of bacterial origin, especially *Acidobacteria* (up to 32% of taxonomically annotated CAZY transcripts). However, this could also be biased by the overrepresentation of bacterial genomes in the reference CAZY database or by the unidentified transcript fraction in our data sets (19 ± 13% of quality filtered sequences; Supplementary Table 2). The high taxonomic diversity of and similarity between taxonomic

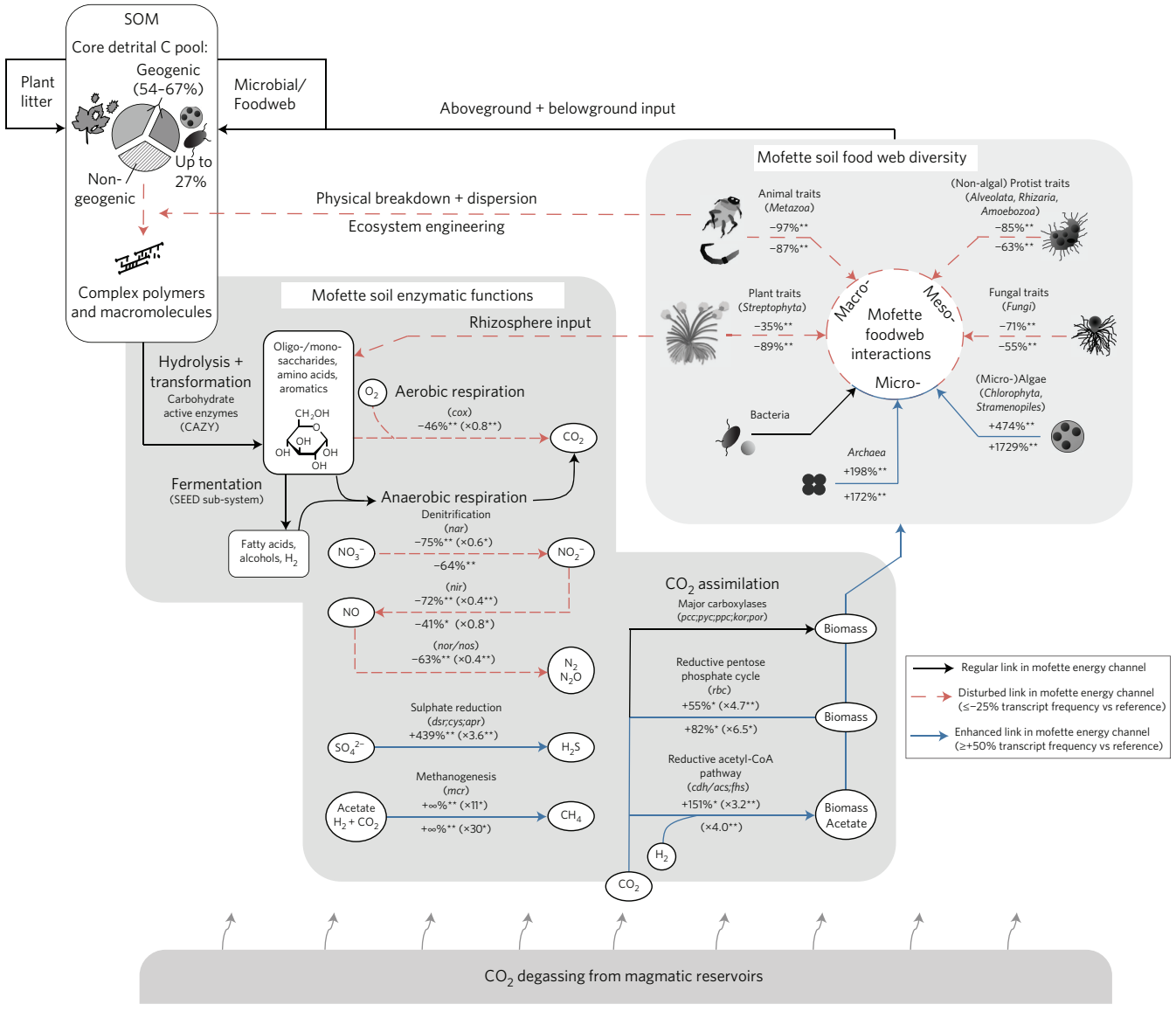

Figure 3 | Conceptual model summarizing the effects of extremely high CO_2 concentration on major wetland floodplain soil enzymatic functions and soil food web diversity, as deduced from metatranscriptomes and metagenomes. Values above arrows (0–10 cm samples) and below arrows (25–40 cm samples) depict the percentage of increased or decreased transcript frequency in mofette relative to reference samples of the same depth (that is, $1-(RNA_{Mofette}/RNA_{Reference})$). Values in brackets depict the estimated average expression in the mofette ($RNA_{Mofette}/DNA_{Mofette}$). Changes in soil food web diversity are deduced from organism-specific changes in the ribo-tag frequency of the metatranscriptomes (see Supplementary Fig. 4). Arrows without values indicate an absence of major differences. SOM inputs depict estimates of plant- and microbially derived primary production based on this work and follow-up investigations[48]. +∞% = not detected in reference; $^*P < 0.05$, $^{**}P < 0.001$ (Welch's *t*-test; $N = 3$). Data are shown as mean ± s.d.

profiles of CAZY transcripts and those related to fermentation (Supplementary Table 3) further suggested a community-wide involvement in anaerobic SOM degradation.

It is possible that transcriptional activity and actual enzyme activity levels are decoupled. For example, redox enzymes working in conjunction with carbohydrate active enzymes (CAZY related class AA), such as ligninolytic enzymes, might be inhibited under oxygen-deprived conditions in the mofette. In fact, a combination of enzyme-mediated mobilization and subsequent retention of ligno-cellulosic breakdown products would provide a feasible explanation for the unusual patterns of increasing C contents with depth in the mofette (Fig. 1). Mineralization of lignin compounds can also proceed under anoxic conditions[25,26]. However, typical preferential transformation of carbohydrate moieties in litter biomass[27] leads to partial disintegration and subsequent solubilization of lignin–hemicellulose networks[28]. Under acidic conditions, like in the mofette, lignin surface charge neutralization (mainly by H^+) facilitates aggregation and eventually precipitation[29].

Impact of volcanic CO_2 degassing on major pathways of C and energy metabolism. Stable, low redox conditions as a result of upstreaming CO_2 appear to enable the activity of strictly anaerobic processes, even at shallow depths near the soil surface (Fig. 3a). For example, we found a remarkable increase in the frequency of transcripts related to methanogenesis (*mcr*) and sulphate reduction (*dsr*, *cys*, *apr*), but a lower frequency of transcripts related to aerobic respiration (*cox*) compared with the reference. Key transcripts of denitrification steps (*nar*, *nir*, *nor*, *nos*) also had a lower frequency in the mofette. A relative increase in transcript frequency was generally also reflected in an increase in the putative expression levels (RNA/DNA), especially for *mcr* transcripts. Similar to CAZY frequency profiles, no major differences in the transcript

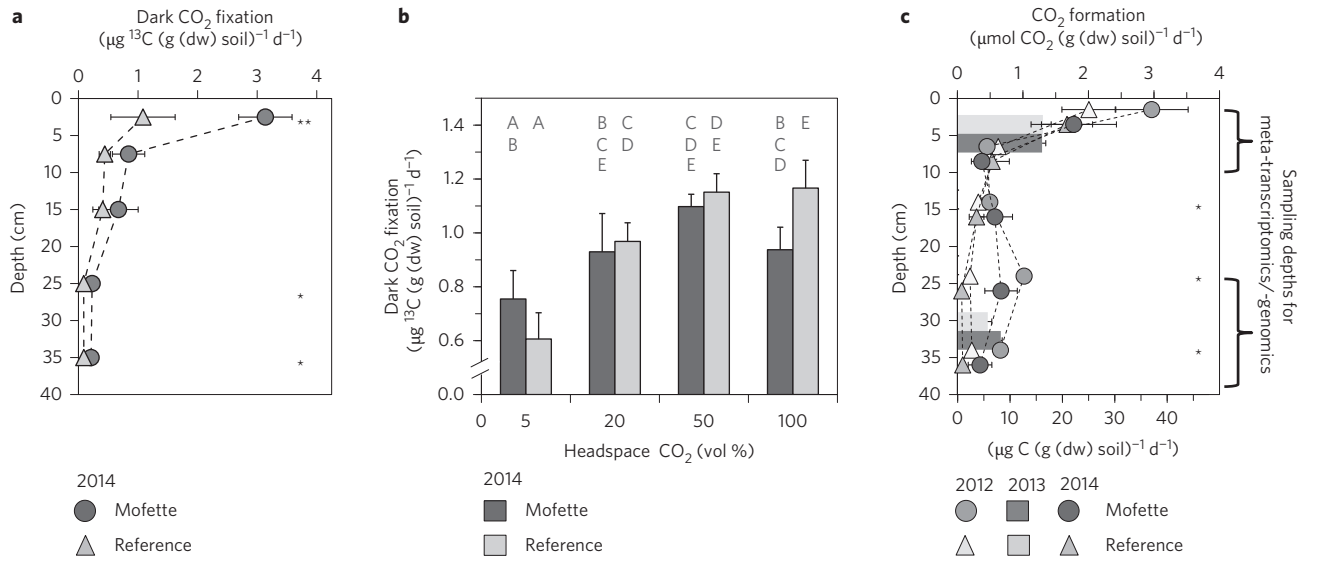

Figure 4 | Rates of CO_2 fixation and formation in mofette and reference soil incubations. a, Rates of dark CO_2 fixation in mofette (100 vol% $^{13}CO_2$; dark grey circles) and reference (5 vol% $^{13}CO_2$, 95 vol% N_2; light grey triangles; $N = 4$). **b**, Effect of CO_2 concentration (5, 20, 50 and 100 vol% $^{13}CO_2$; $N = 4$) on rates of dark CO_2 fixation in mofette (dark grey bars) and reference (light grey bars). Values with the same letter are not significantly different from each other (Tukey–Kramer test, $P > 0.05$). **c**, Rates of aerobic (air; only reference 0–10 cm) and anaerobic CO_2 formation (100 vol% N_2) in mofette (grey circles) and reference (grey triangles) during yearly sampling campaigns (different grey shades, $N = 3$). Data points from the same sampling depths but different years are slightly displaced from each other for clearer illustration; $^*P < 0.05$, $^{**}P < 0.001$ (Welch's t-test). All data are shown as mean ± s.d.

abundance of individual SEED fermentation subsystems were detected between mofette and reference, suggesting that, on the community scale, fermentative C turnover was largely unaffected by high $p(CO_2)$.

Consistent with the strong geogenic signature in mofette SOM, we detected high frequencies of transcripts encoding key enzymes of the autotrophic Calvin cycle and reductive acetyl-CoA pathway. The latter is found in acetogens and non-acetogens, for example, methanogens and sulphate reducers, and the enzymes involved are used anabolically or catabolically for CO_2 reduction or acetate oxidation, respectively[30]. Transcripts of the key enzyme complex CO dehydrogenase/acetyl-CoA synthase (encoded by *cdh*/*acs*) were primarily related to *Clostridia* (phylum *Firmicutes*; up to 33%) harbouring numerous acetogens[30], methanogenic *Methano-microbiales* (phylum *Euryarchaeota*; up to 27%) and the presumably sulphate-reducing or syntrophic *Syntrophobacterales* (class *Deltaproteobacteria*; up to 34%)[31] (Supplementary Table 4). Transcripts of the Calvin cycle key enzyme ribulose-1,5-bisphosphate carboxylase/oxygenase (Rubisco, encoded by *rbc*) in the mofette were primarily related to *Chlorophyta* and *Bacillariophyta* algae (*Chlorophyta* and *Stramenopiles*; up to 60% of *rbc* transcripts) and showed up to four times higher potential expression levels (RNA/DNA) than reference samples, in which no algae-related *rbc* transcripts were detected. Under anoxic and non-phototrophic conditions, algae might generate ATP via mitochondrial respiration or fermentation[32], and this energy could fuel CO_2 assimilation via the Calvin cycle[33]. Under atmospheric CO_2 concentrations, most algae depend on energetically intensive CO_2-concentrating mechanisms to cope with the competition between O_2 and CO_2 for the active sites of Rubisco[34]. Thus, adapted algae and also other autotrophs in the mofette might profit energetically from the high CO_2 concentrations.

Impact of volcanic CO_2 degassing on soil diversity and functions. A three-domain taxonomic profile of small subunit rRNA sequences (SSU ribo-tags) revealed that bacterial ribo-tags represented the highest fraction in all metatranscriptomes (83–91%; Supplementary Fig. 2). Most archaeal ribo-tags (up to 6%) were found at a depth of 25–40 cm in the mofette, whereas most eukaryotic ribo-tags (up to 16%) were found in the 0–10 cm depth of the reference. 16S rRNA gene copy numbers decreased only slightly with depth and were similar overall for Bacteria in both soils (~10^9 to 10^{10} genes (g (dw) soil)$^{-1}$; Supplementary Table 1) and slightly higher in the mofette for Archaea (>10^9 genes (g (dw) soil^{-1}) than in the reference (~10^8 to 10^9 genes (g (dw) soil)$^{-1}$). This suggested that the observed relative changes in our metatranscriptome and -genome data could be representative of shifts to more specialized functional groups, rather than an increase in overall biomass.

Shannon and ACE (abundance-based coverage estimator) richness estimators indicated substantially lower phylogenetic diversity in the mofette than in the reference for all three domains of life. This was also reflected in a substantially lowered richness of general functional genes and transcripts (as indicated by fewer Kyoto Encyclopedia of Genes and Genomes (KEGG) database and Protein families (Pfam) database features in mofette samples), but not for carbon degradation (as indicated by a similar richness of CAZY annotations; Supplementary Fig. 3). Differences in functional richness between mofette and reference were found in both metatranscriptomes and metagenomes, suggesting mid- to long-term diversity effects of extreme CO_2 exposure for general metabolic functions, and these differences were highest at shallow depths near the soil surface. As a potential analogue to the functional traits of meso- to macroscopic organisms, lowered metabolic complexity caused by high CO_2 levels could be associated with decreased facilitative interactions within the soil biome[35]. This might have detrimental consequences for the resilience and/or efficiency of the mofette soil food web and SOM processing.

As is typical for wetlands[36,37], the reference eukaryotic community was highly diverse and represented by animals (*Metazoa*, up to 25%; primarily *Annelida* and *Hexapoda*), plants (*Streptophyta*, up to 13%), different protists (up to 24%; *Alveolata*, *Rhizaria* and *Amoebozoa*) and fungi (up to 47%; *Ascomycota*, *Basidiomycota* and *Glomeromycota*) (Fig. 3b). In contrast, high fractions of algae (up to 60%; primarily *Trebouxiophyceae* within *Chlorophyta*, as well as *Chrysophycaea* and *Bacillariophyta* within *Stramenopiles*) together with *Ascomycota* dominated the eukaryotes in the mofette. Their presence, especially in deeper layers, might be

indicative of an anaerobic and heterotrophic lifestyle[32], as some algae can tolerate up to ~100% CO_2[38]. Long-term exposure to the altered environmental conditions might have allowed their enrichment along with the potential generation of phenotypic heterogeneity or even invasion of adapted species. In contrast, the much lower frequency of organisms belonging to higher trophic levels (animals and protists), putative myccorhizal fungi and plants suggests that pivotal soil food web interactions and functions associated with the activity of these organisms were likely to be missing or severely impaired. These include the physical (for example, litter breakdown and accessibility) and ecological (for example, predation, mutualistic benefits from myccorhizal associations) traits that allow for efficient SOM decomposition and therefore would explain the preservation of less-degraded organic matter[39].

The composition of the bacterial community at the class level was fairly similar in both soils and depths (Supplementary Fig. 2), suggesting that these are well adapted to changes in pH and redox conditions, for example, due to degassing CO_2 or a fluctuating water table. Most ribo-tags belonged to Subdivision 1 *Acidobacteria* (25–43%), followed by *Deltaproteobacteria* (13–21%). *Acidobacteria* in particular were considered to be involved in SOM degradation due to their rich enzymatic capabilities to degrade complex organic material[40]. Most *Deltaproteobacteria* belonged to the potentially sulphate-reducing or syntrophic *Syntrophaceae* (up to 13%)[31] in the mofette or to the mobile and micropredatory *Myxococcales* (up to 16%)[41] in the reference. Archaeal ribo-tags of the mofette were dominated by the H_2–CO_2-using *Methanoregulaceae* and acetate-using *Methanosaetaceae* of the *Methanomicrobiales* (21–47%)[42,43], as well as putative anaerobic and heterotrophic members of the MCG (Miscellaneous Crenarchaeotal Group, 33–43%)[44].

Importance of subsurface CO_2 utilization for soil C storage. Because of the molecular evidence for augmented CO_2 utilization and strong geogenic signatures in mofette SOM (Fig. 1), we tested the depth-resolved potentials for dark CO_2 fixation with $^{13}CO_2$-labelling incubations close to *in situ* CO_2 concentrations (5 vol% in the reference and 100 vol% in the mofette; Fig. 4a). Dark CO_2 fixation was generally higher in the mofette (1.5–3 times), with up to 3.14 ± 0.44 μg ^{13}C (g (dw) soil)$^{-1}$ d^{-1} (0–10 cm) and decreased strongly with depth in both soils. Assuming a bulk density of 1 g cm^{-3} and that the observed incorporation rates for each respective depth interval remain constant, microorganisms can potentially fix 0.29 ± 0.07 g C m^2 d^{-1} in the mofette and 0.13 ± 0.05 g C m^2 d^{-1} in the reference. Compared with a typical primary production of ~0.3–12 g C m^2 d^{-1} in *Eriophorum*-dominated wetlands[45–47], dark CO_2 fixation could contribute a substantial fraction of soil C input, especially near the soil surface. Detailed follow-up investigations using comparative radiocarbon and stable carbon isotope ratio analysis confirmed the importance of subsurface CO_2 assimilation, with an estimated microbial contribution to the geogenic C input of up to ~27% in the SOM of the mofette[48].

We also tested the effect of CO_2 concentrations (5, 20, 50 and 100 vol%) on dark CO_2 fixation. Even in the reference soil, dark CO_2 fixation increased 1.4- to 2-fold from 5 to 50 vol% CO_2 (Fig. 2b) and demonstrated the ability of biota in both soils to respond to short-term (≤14 days) changes in gas composition. Moreover, an intriguing similarity to Michaelis–Menten kinetics suggested subjection to enzymatic limitations, that is, substrate concentration and saturation. This provided a feasible explanation for the difference in depth-resolved dark CO_2 fixation between the soils at close to *in situ* CO_2 concentrations (Fig. 2a). The significance of high CO_2 concentrations (>5 vol%) for CO_2 utilization in soils has generally been overlooked. Considering the regular variability of $p(CO_2)$ in soil pore space over several orders of magnitude (up to ~10 vol%[49]), for example during bad aeration, our observations point to a quantitative input with relevance also for C (re-)cycling in other soils[50].

To relate the increased dark CO_2 fixation to the CO_2 released by decomposition, we investigated the mofette and reference soil with depth-resolved anoxic and oxic incubation studies (Fig. 2c). CO_2 production was at least 5.7 times higher than dark CO_2 fixation, indicating that dark CO_2 fixation alone could not sustain the mofette C and that the major fraction of 'volcanic' soil C originated from plant litter input. Furthermore, CO_2 production was similarly high at all depths of mofette (3.0 ± 0.2 to 35.6 ± 6.7 μg C (g (dw) soil)$^{-1}$ d^{-1}) and reference (1.0 ± 0.5 to 24.1 ± 4.9 μg C (g (dw) soil)$^{-1}$ d^{-1}). Exoenzymatic activity estimators (β-glucosidase, cellobiosidase and general hydrolysing enzyme activity; Supplementary Fig. 4) also indicated similar to higher activities in the mofette compared with the reference and, consistent with the metatranscriptome and metagenome data, further pointed to an unimpaired biochemical potential for SOM mineralization in the mofette. At this point it is worth noting that, despite the overall consistency between mofette geochemistry and transcriptional activity, further investigation of actual enzyme activities under *in situ* conditions is needed, because end-product inhibition could become relevant at high CO_2 concentrations, for example.

Concluding remarks

The studied mofette presents a unique and extreme soil environment that harbours various groups of microorganisms adapted to long-term high CO_2 exposure. CO_2-utilizing anaerobes and algae in particular seem to profit from these conditions and continuously introduce CO_2 emanating from the Earth's mantle into the soil C cycle. CO_2 exposure not only affects soil diversity, but also food web structure, leading to the exclusion of higher trophic levels and associated physical and ecological traits, which has allowed for the preservation of old (geogenic), less degraded organic matter and even pieces of intact plant structures. Almost complete reduction of the soil community to levels of microbial primary production and consumption makes the mofette a model environment for studying diversity effects on specific soil functions. The evidence supporting highly similar biochemical potentials of SOM degradation in the mofette and reference was surprising and implied a degree of redundancy in soil biomes for specific enzymatic traits. Our study yielded testable predictions about the influence of extreme CO_2 concentrations on metabolisms of various functional groups and demonstrated how an integrated molecular and biogeochemical approach provides novel insights into the complex relationships between soil communities and the regulation of soil C dynamics.

Methods

Site description, sampling design and soil classification. The studied mofette and reference soils were located in the flood plain of the River Plesná (50°08′48.4″N, 12°27′04.5″E; Počatky–Plesná fault zone between Hartoušov and Milhostov, Czech Republic) and investigated over the course of three annual sampling campaigns in 2012 to 2014. Post-volcanic activity and deep tectonic faults in the Cheb Basin led to continuous mantle-derived CO_2 degassings, most prominently in the form of mofettes. Due to hydric soil conditions, mofettes could be easily identified by visible gas streams at the soil surface. CO_2-unaffected floodplain reference sites in close proximity (<5 m distance) were selected based on their location between mofette-specific vegetation (mainly *Deschampsia cespitosa* and *Eriophorum vaginatum*) and typical floodplain vegetation (mainly *Filipendula ulmaria*). The absence of CO_2 emissions in reference soils was verified with a portable infrared gas analyser (GA2000, Ansyco). In July 2012 we performed soil classification and bulk soil geochemical analysis and assayed the soil microbial activity estimators CO_2 formation and exoenzymatic activities. In July 2013 we sampled for metatranscriptome and metagenome analysis and assayed soil microbial activity estimators in parallel. In May 2014 we studied depth-resolved potentials for CO_2 fixation and CO_2 formation. The average air temperatures of 15 °C were similar in 2012, 2013 and 2014, but the total precipitation of 100 mm in 2013 was higher than in 2012 and 2014 (80 mm; CHMI, http://www.chmi.cz). Mofette and reference soils were classified according to the World Reference Base (WRB) for Soil Resources[51] as well as the German soil classification system[52], because the WRB does not consider

the influence of geogenic CO_2 as a parameter of soil formation. To prevent disturbance of the studied mofette and wetland reference soils, pits for soil classification (2012) were dug at an adjacent mofette field (<50 m distance) and compared to soil cores of the study site. Topsoil (A horizon; with geogenic prefix 'a' for flood plain dynamics, and pedogenic suffixes 'a' for hydric conditions and humic enrichment) was underlain by either horizons under the influence of reducing gases in the mofette soil (Y horizon) or a fluctuating water table in the reference soil (G horizons; with geogenic prefix 'o' for organic, and pedogenic suffixes 'h' for humic enrichment, 'o' for oxidized and 'r' for reduced conditions). Mofette and reference soils both had primarily single grain to massive (coherent) soil structure throughout. Blocky soil peds were also observed in deeper parts of the reference (23–37 cm and 40–58 cm depth). The particle size of the mineral fraction transitioned from silty loam to silty clay at greater depths (≥13 cm depth in the mofette and ≥23 cm depth in the reference).

Soil sampling, geochemical analysis and exoenzymatic activity potentials. Soil samples were generally obtained in the form of three biological replicates with an auger (1.7 or 8 cm diameter) and transported at 4 °C under an Ar-headspace or immediately frozen in the field with liquid N_2 and stored at −80 °C until nucleic acid extraction. Before each sampling, 0–2 cm of the soil, mainly composed of litter, was removed. Pore water was extracted from the soil samples by centrifugation at 10,000*g* for 10 min. Redox potential, pH, sulphate (SO_4^{2-}), nitrate (NO_3^-) and ferrous iron (Fe^{2+}) concentrations were measured as described previously[8]. TGA of bulk soil and quantification of C and N were performed with air-dried and milled (ball mill MM 200, Retsch) soil samples, as described previously[53]. The dispersion of TGA mass loss as well as C and N contents between replicates were tested for each soil, and standard deviations were <0.1% ($N = 3$). The TOC and its stable carbon isotopic composition ($\delta^{13}C$) were analysed by continuous-flow elemental analyser–isotope ratio mass spectrometry (EA-IRMS), as described previously[54]. All isotope ratios are given in $\delta^{13}C$ notation (per mil, ‰) relative to the Vienna Peedee Belemnite Standard (VPDB), where $\delta^{13}C = [(R_{sample} - R_{VPDB})/R_{VPDB}] \times 10^3$, with $R = {}^{13}C/{}^{12}C$ and $R_{VPDB} = 0.0112372 \pm 2.9 \times 10^{-6}$. Radiocarbon concentrations of soil and plant tissue samples were determined by accelerator mass spectrometry (AMS) in the Jena ^{14}C facilities[55]. Subsamples of soil or plant tissues containing 1 mg C were combusted quantitatively, and the developed CO_2 was catalytically reduced to graphite at 625 °C by H_2 reduction. The analytical precision of radiocarbon measurements was better than 3‰ and is reported as [pMC][56]. Activities of phosphatases, β-glucosidases, general hydrolases (lipases, esterases and proteases) and β-exoglucanase (cellulase) were determined for 0.1 g ml^{-1} soil suspensions at a predetermined substrate saturation using the model substrates methylumbelliferyl phosphate (MUF-P, 1 mM), methylumbelliferyl-β-gluco-pyranoside (MUF-β-Glc, 1.5 mM), diacetyl-fluorescein (FDA, 57 μM) and methylumbelliferyl-β-cellobiose (MUF-β-Cel, 287m μM), as described previously[57–59]. Absorption and fluorescence were measured using a DR 3800 spectrophotometer (Hach Lange) and a Quantifluor-ST fluorometer (Promega), respectively. Enzyme kinetic parameters, blank controls and matrix effects, that is, sorption of the dye to soil particles, were determined for each soil and substrate.

(An-)aerobic CO_2 production and fixation. Microcosms were constructed by adding 5–10 g (wet weight, ww) replicate soil material to sterile 150 ml incubation flasks (Mueller and Krempel) in a chamber filled with >99 vol% N_2 and pre-incubated for ~1 day in the dark at 12 °C. For depth-resolved potentials of CO_2 formation, the flask gas phase was flushed with sterile N_2 (for anoxic incubations) or sterile air (for oxic incubations) and incubated statically in the dark at 12 °C. Evolved CO_2 was measured by gas chromatography as described previously[53]. For depth-resolved potentials of CO_2 fixation, the flask gas phase was adjusted to close to *in situ* compositions with 5% $^{13}CO_2$ and 95% N_2 for reference soil samples and 100% $^{13}CO_2$ for mofette soil samples, and incubated statically in the dark at 12 °C. ^{13}C incorporations into the bulk soil after 14 days of incubation were measured as described previously[8].

Nucleic acid extraction and processing, and Illumina sequencing. Total nucleic acids were extracted from ~0.6 g soil (oven-dried equivalent weight, soil was not dried before extraction), according to a protocol described previously[60]. Raw extracts contained high amounts of co-extracted organic soil compounds. These contaminants were removed by sequential purification with gel columns (S-400 HR, Zymo Research) and silica columns (Powersoil Total RNA Kit in combination with the DNA Elution Accessory kit, MO BIO Laboratories). Total nucleic acid extraction efficiency, quantified using a Nanodrop 1000 spectrophotometer (Thermo Scientific), was similar between respective depths of mofette and reference (Supplementary Table 1). For each of the following steps, DNA and RNA concentrations were quantified fluorometrically with the dsDNA and RNA System from Promega GmbH, and quality was checked by agarose gel electrophoresis. In samples for metatranscriptomic and -genomic analysis, DNA or RNA were digested using 6 units Ambion TURBO DNase I (life technologies) or 300 units RNase I_f (New England Biolabs), respectively. Reactions were stopped with the supplied Ambion DNase inactivation reagent or by heat inactivation of RNase I_f for 10 min at 70 °C. Nucleic acids were then extracted with phenol:chloroform:isoamylalcohol (25:24:1, vol:vol:vol; Sigma Aldrich) and chloroform:isoamylalcohol (24:1, vol:vol; Sigma Aldrich) followed by poly(ethylene glycol) 8000 (Sigma Aldrich) precipitation. Purified RNA (200 ng) was used as a template for whole-RNA amplification and *in vitro* transcription using the Ambion MessageAmp II aRNA Kit (Life Technologies), according to the manufacturer's instructions. RNA was then subjected to reverse transcription using the Superscript II double-strand complementary DNA synthesis kit (Invitrogen), following the manufacturer's protocol, with the exceptions that 3 μl Superscript II RT was used and both first- and second-strand syntheses were carried out for 2 h. The resulting double-stranded cDNA was extracted with phenol:chloroform:isoamylalcohol and chloroform: isoamylalcohol followed by poly(ethylene glycol) 8000 precipitation. DNA and cDNA samples were converted to Illumina-compatible sequencing libraries using the SPRIworks system (Beckman Coulter), employing TruSeq oligonucleotide adapters (Illumina) and 10 or 12 cycles of PCR amplification for DNA and cDNA, respectively. Libraries were then subjected to size-selection by agarose gel eletrophoresis to enrich molecules with insert sizes in the 150–190 bp range. Libraries were pooled and sequenced over two lanes of a HiSeq 2500 (Illumina), employing 100 bp paired-end reads with SBS v3 reagents. Copy numbers of archaeal and bacterial 16S rRNA genes in DNA were determined by quantitative PCR on an Mx3005P instrument (Agilent) by using the primer combinations Bac908F_mod/Bac1075R for bacteria and 915Fmod/1059R for Archaea[61].

Bioinformatic analysis. Metagenomic and metatranscriptomic llumina raw reads were quality filtered, assembled and initially screened using the metagenomics (MG)-RAST server[62]. Post quality control reads (79 ± 4% of the original data set resulting in $8.92 \pm 0.82 \times 10^6$ reads per sample and a length of 160 ± 26 bp) were downloaded and clustered at 90% nucleic acid similarity with CD-HIT[63]. Further data-handling involved custom Linux Shell and PERL scripts, which are available from the authors on request. Putative rRNA reads were identified by BLASTN searches (bitscore > 50) and BWA mapping[64] against a modified SILVA SSU database[65], as well as the SILVA SSU and LSU rRNA reference databases[66]. SSU BLASTN reads were analysed with MEGAN (parameters: min. bit score 150, min. support 1, top percent 10; 50 best blast hits)[67]. For diversity estimation[68], SSU rRNA reads were randomly subsampled and normalized to 7,500 sequences per sample, as well as 15,000 domain-specific sequences (*Bacteria*, *Archaea* or *Eukaryota* annotation) per sample. Diversity estimation was based on CREST taxonomy level classifications. The remaining putative mRNA reads were translated into six reading frames. To identify protein coding features, open reading frames (ORFs) ≥ 40 amino acids were inspected by reference HMMs (hidden Markov models) using HMMER tools (http://hmmer.janelia.org/; *e*-value < 1 e^{-4}) with PFAM HMMs (PFAM-A release 27; http://pfam.janelia.org), as well as CAZY HMMs[69]. Additional screening of protein coding sequences for specific functional genes and transcripts was carried out with RAPSearch2 (*e*-value < 1 e^{-4})[70] against the NCBI RefSeq (http://www.ncbi.nlm.nih.gov/refseq/) protein database and custom reference databases of MD5nr, KEGG and FIGfam sequences retrieved from the SEED servers (http://www.theseed.org). Sequences were taxonomically binned using NCBI taxonomy mapping. For diversity estimation, mRNA reads were randomly subsampled and normalized according to the lowest amount of annotated protein coding sequences.

Accession numbers. The sequences reported in this paper have been deposited in the Sequence Read Archive (SRA) database, www.ncbi.nlm.nih.gov/sra (accession numbers SRX1030315–SRX1030319 and SRX1030268).

Received 13 August 2015; accepted 8 December 2015; published 27 January 2016; corrected 11 February 2016

References

1. Kämpf, H., Bräuer, K., Schumann, J., Hahne, K. & Strauch, G. CO_2 discharge in an active, non-volcanic continental rift area (Czech Republic): characterisation ($\delta^{13}C$, $^3He/^4He$) and quantification of diffuse and vent CO_2 emissions. *Chem. Geol.* **339,** 71–83 (2013).
2. Emiliani, C. *Planet Earth: Cosmology, Geology, and the Evolution of Life and Environment* (Cambridge Univ. Press, 1992).
3. Raven, J. A. The early evolution of land plants: aquatic ancestors and atmospheric interactions. *Bot. J. Scotl.* **47,** 151–175 (1995).
4. Young, J. N., Rickaby, R. E. M., Kapralov, M. V. & Filatov, D. A. Adaptive signals in algal RuBisCO reveal a history of ancient atmospheric carbon dioxide. *Phil. Trans. R. Soc. Lond. B* **367,** 483–492 (2012).
5. Blume, H.-P. & Felix-Henningsen, P. Reductosols: natural soils and technosols under reducing conditions without an aquic moisture regime. *J. Plant Nutr. Soil Sci.* **172,** 808–820 (2009).
6. Mehlhorn, J., Beulig, F., Küsel, K. & Planer-Friedrich, B. Carbon dioxide triggered metal(loid) mobilisation in a mofette. *Chem. Geol.* **382,** 54–66 (2014).
7. Rennert, T., Eusterhues, K., Pfanz, H. & Totsche, K. U. Influence of geogenic CO_2 on mineral and organic soil constituents on a mofette site in the NW Czech Republic. *Eur. J. Soil Sci.* **62,** 572–580 (2011).
8. Beulig, F. *et al.* Carbon flow from volcanic CO_2 into soil microbial communities of a wetland mofette. *ISME J.* **9,** 746–759 (2015).
9. McInerney, M. J. & Bryant, M. P. in *Biomass Conversion Processes for Energy and Fuels* (eds Sofer, S. S. & Zaborsky, O. R.) 277–296 (Springer, 1981).

10. Ekschmitt, K. *et al.* Soil-carbon preservation through habitat constraints and biological limitations on decomposer activity. *J. Plant Nutr. Soil Sci.* **171,** 27–35 (2008).
11. Burns, R. G. *et al.* Soil enzymes in a changing environment: current knowledge and future directions. *Soil Biol. Biochem.* **58,** 216–234 (2013).
12. Urich, T. *et al.* Simultaneous assessment of soil microbial community structure and function through analysis of the meta-transcriptome. *PLoS ONE* **3,** e2527 (2008).
13. Tveit, A., Schwacke, R., Svenning, M. M. & Urich, T. Organic carbon transformations in high-Arctic peat soils: key functions and microorganisms. *ISME J.* **7,** 299–311 (2013).
14. Tveit, A. T., Urich, T., Frenzel, P. & Svenning, M. M. Metabolic and trophic interactions modulate methane production by Arctic peat microbiota in response to warming. *Proc. Natl Acad. Sci. USA* **112,** E2507–E2516 (2015).
15. Hultman, J. *et al.* Multi-omics of permafrost, active layer and thermokarst bog soil microbiomes. *Nature* **521,** 208–212 (2015).
16. Nieder, R. & Benbi, D. K. *Carbon and Nitrogen in the Terrestrial Environment* (Springer, 2008).
17. Schrumpf, M. *et al.* Storage and stability of organic carbon in soils as related to depth, occlusion within aggregates, and attachment to minerals. *Biogeosciences* **10,** 1675–1691 (2013).
18. Gleixner, G., Danier, H.-J., Werner, R. A. & Schmidt, H.-L. Correlations between the ^{13}C content of primary and secondary plant products in different cell compartments and that in decomposing *Basidiomycetes*. *Plant Physiol.* **102,** 1287–1290 (1993).
19. Werth, M. & Kuzyakov, Y. ^{13}C fractionation at the root–microorganisms–soil interface: a review and outlook for partitioning studies. *Soil Biol. Biochem.* **42,** 1372–1384 (2010).
20. Conrad, R. Quantification of methanogenic pathways using stable carbon isotopic signatures: a review and a proposal. *Org. Geochem.* **36,** 739–752 (2005).
21. Heuer, V. B., Pohlman, J. W., Torres, M. E., Elvert, M. & Hinrichs, K.-U. The stable carbon isotope biogeochemistry of acetate and other dissolved carbon species in deep subseafloor sediments at the northern Cascadia Margin. *Geochim. Cosmochim. Acta* **73,** 3323–3336 (2009).
22. Rubino, M. *et al.* An isotopic method for testing the influence of leaf litter quality on carbon fluxes during decomposition. *Oecologia* **154,** 155–166 (2007).
23. Kleber, M., Mikutta, R., Torn, M. S. & Jahn, R. Poorly crystalline mineral phases protect organic matter in acid subsoil horizons. *Eur. J. Soil Sci.* **56,** 717–725 (2005).
24. Schneider, T. *et al.* Who is who in litter decomposition? Metaproteomics reveals major microbial players and their biogeochemical functions. *ISME J.* **6,** 1749–1762 (2012).
25. Benner, R., Maccubbin, A. E. & Hodson, R. E. Anaerobic biodegradation of the lignin and polysaccharide components of lignocellulose and synthetic lignin by sediment microflora. *Appl. Environ. Microbiol.* **47,** 998–1004 (1984).
26. Deangelis, K. M. *et al.* Evidence supporting dissimilatory and assimilatory lignin degradation in *Enterobacter lignolyticus* SCF1. *Front. Microbiol.* **4,** 280 (2013).
27. Breznak, J. A. & Brune, A. Role of microorganisms in the digestion of lignocellulose by termites. *Annu. Rev. Entomol.* **39,** 453–487 (1994).
28. McSweeney, C. S., Dulieu, A., Katayama, Y. & Lowry, J. B. Solubilization of lignin by the ruminal anaerobic fungus *Neocallimastix patriciarum*. *Appl. Environ. Microbiol.* **60,** 2985–2989 (1994).
29. García, A. *et al.* Characterization of lignins obtained by selective precipitation. *Sep. Purif. Technol.* **68,** 193–198 (2009).
30. Drake, L., Küsel, K. & Matthies, C. Acetogenic prokaryotes. *Prokaryotes Prokaryotic Physiol. Biochem*. 3–60 (2013).
31. Kuever, J. in *The Prokaryotes* (eds Rosenberg, E., DeLong, E. F., Lory, S., Stackebrandt, E. & Thompson, F.) 281–288 (Springer, 2014).
32. Müller, M. *et al.* Biochemistry and evolution of anaerobic energy metabolism in eukaryotes. *Microbiol. Mol. Biol. Rev. MMBR* **76,** 444–495 (2012).
33. Subramanian, V. *et al.* Profiling *Chlamydomonas* metabolism under dark, anoxic H_2-producing conditions using a combined proteomic, transcriptomic, and metabolomic approach. *J. Proteome Res.* **13,** 5431–5451 (2014).
34. Giordano, M., Beardall, J. & Raven, J. A. CO_2 concentrating mechanisms in algae: mechanisms, environmental modulation, and evolution. *Annu. Rev. Plant Biol.* **56,** 99–131 (2005).
35. Cardinale, B. J., Palmer, M. A. & Collins, S. L. Species diversity enhances ecosystem functioning through interspecific facilitation. *Nature* **415,** 426–429 (2002).
36. Lara, E., Mitchell, E. A. D., Moreira, D. & López García, P. Highly diverse and seasonally dynamic protist community in a pristine peat bog. *Protist* **162,** 14–32 (2011).
37. Van der Valk, A. G. *The Biology of Freshwater Wetlands* (Oxford Univ. Press, 2012).
38. Salih, F. M. Microalgae tolerance to high concentrations of carbon dioxide: a review. *J. Environ. Prot.* **2,** 648–654 (2011).
39. Gessner, M. O. *et al.* Diversity meets decomposition. *Trends Ecol. Evol.* **25,** 372–380 (2010).
40. Ward, N. L. *et al.* Three genomes from the phylum *Acidobacteria* provide insight into the lifestyles of these microorganisms in soils. *Appl. Environ. Microbiol.* **75,** 2046–2056 (2009).
41. Kuever, J., Rainey, F. A. & Widdel, F. in *Bergey's Manual® of Systematic Bacteriology* (eds Brenner, D. J., Krieg, N. R. & Staley, J. T.) 922–1144 (Springer, 2005).
42. Bräuer, S. L., Cadillo-Quiroz, H., Ward, R. J., Yavitt, J. B. & Zinder, S. H. *Methanoregula boonei* gen. nov., sp. nov., an acidiphilic methanogen isolated from an acidic peat bog. *Int. J. Syst. Evol. Microbiol.* **61,** 45–52 (2011).
43. Whitman, W., Boone, D., Koga, Y. & Keswani, J. Taxonomy of methanogenic archaea. *Bergey's Manual Syst. Bacteriol.* 211–294 (2001).
44. Kubo, K. *et al.* Archaea of the Miscellaneous Crenarchaeotal Group are abundant, diverse and widespread in marine sediments. *ISME J.* **6,** 1949–1965 (2012).
45. Lindroth, A. *et al.* Environmental controls on the CO_2 exchange in north European mires. *Tellus B* **59,** 812–825 (2007).
46. Waddington, J. M. & Roulet, N. T. Carbon balance of a boreal patterned peatland. *Glob. Change Biol.* **6,** 87–97 (2000).
47. Wu, J., Roulet, N. T., Sagerfors, J. & Nilsson, M. B. Simulation of six years of carbon fluxes for a sedge-dominated oligotrophic minerogenic peatland in Northern Sweden using the McGill Wetland Model (MWM). *J. Geophys. Res. Biogeosci.* **118,** 795–807 (2013).
48. Nowak, M. *et al.* Autotrophic fixation of geogenic CO_2 by microorganisms contributes to soil organic matter formation and alters isotope signatures in a wetland mofette. *Biogeosci. Discuss.* **12,** 14555–14592 (2015).
49. Mückenhausen, E. *Die Bodenkunde und ihre geologischen, geomorphologischen und petrologischen Grundlagen* (DLG-Verlag, 1993).
50. Kramer, C. & Gleixner, G. Variable use of plant- and soil-derived carbon by microorganisms in agricultural soils. *Soil Biol. Biochem.* **38,** 3267–3278 (2006).
51. IUSS Working Group WRB. *World Reference Base for Soil Resources 2006*. World Soil Resources Report No. 103 (FAO, 2006).
52. Ad-Hoc-AG Boden. *Bodenkundliche Kartieranleitung* 5th edn (Schweitzerbart'sche Verlagsbuchhandlung, 2005).
53. Reiche, M., Gleixner, G. & Küsel, K. Effect of peat quality on microbial greenhouse gas formation in an acidic fen. *Biogeosciences* **7,** 187–198 (2010).
54. Steinbeiss, S., Temperton, V. M. & Gleixner, G. Mechanisms of short-term soil carbon storage in experimental grasslands. *Soil Biol. Biochem.* **40,** 2634–2642 (2008).
55. Steinhof, A., Adamiec, G., Gleixner, G., Wagner, T. & van Klinken, G. The new ^{14}C analysis laboratory in Jena, Germany. *Radiocarbon* **46,** 51–58 (2007).
56. Mook, W. G. & van der Plicht, J. Reporting ^{14}C activities and concentrations. *Radiocarbon* **41,** 227–239 (2006).
57. Reiche, M., Hädrich, A., Lischeid, G. & Küsel, K. Impact of manipulated drought and heavy rainfall events on peat mineralization processes and source-sink functions of an acidic fen. *J. Geophys. Res. Biogeosci.* **114,** G02021 (2009).
58. Boschker, H. T. & Cappenberg, T. E. A sensitive method using 4-methylumbelliferyl-β-cellobiose as a substrate to measure (1,4)-β-glucanase activity in sediments. *Appl. Environ. Microbiol.* **60,** 3592–3596 (1994).
59. Kang, H. & Freeman, C. Measurement of cellulase and xylosidase activities in peat using a sensitive fluorogenic compound assay. *Commun. Soil Sci. Plant Anal.* **29,** 2769–2774 (1998).
60. Lueders, T., Manefield, M. & Friedrich, M. W. Enhanced sensitivity of DNA- and rRNA-based stable isotope probing by fractionation and quantitative analysis of isopycnic centrifugation gradients. *Environ. Microbiol.* **6,** 73–78 (2004).
61. Lever, M. A. *et al.* A modular method for the extraction of DNA and RNA, and the separation of DNA pools from diverse environmental sample types. *Front. Microbiol.* **6,** 476 (2015).
62. Meyer, F. *et al.* The metagenomics RAST server—a public resource for the automatic phylogenetic and functional analysis of metagenomes. *BMC Bioinformatics* **9,** 1–8 (2008).
63. Fu, L., Niu, B., Zhu, Z., Wu, S. & Li, W. CD-HIT: accelerated for clustering the next-generation sequencing data. *Bioinformatics* **28,** 3150–3152 (2012).
64. Li, H. & Durbin, R. Fast and accurate short read alignment with Burrows–Wheeler transform. *Bioinformatics* **25,** 1754–1760 (2009).
65. Lanzén, A. *et al.* CREST—classification resources for environmental sequence tags. *PLoS ONE* **7,** e49334 (2012).
66. Pruesse, E. *et al.* SILVA: a comprehensive online resource for quality checked and aligned ribosomal RNA sequence data compatible with ARB. *Nucleic Acids Res.* **35,** 7188–7196 (2007).
67. Huson, D. H., Auch, A. F., Qi, J. & Schuster, S. C. MEGAN analysis of metagenomic data. *Genome Res.* **17,** 377–386 (2007).
68. Hughes, J. B., Hellmann, J. J., Ricketts, T. H. & Bohannan, B. J. M. Counting the uncountable: statistical approaches to estimating microbial diversity. *Appl. Environ. Microbiol.* **67,** 4399–4406 (2001).
69. Yin, Y. *et al.* dbCAN: a web resource for automated carbohydrate-active enzyme annotation. *Nucleic Acids Res.* **40,** W445–W451 (2012).
70. Zhao, Y., Tang, H. & Ye, Y. RAPSearch2: a fast and memory-efficient protein similarity search tool for next-generation sequencing data. *Bioinformatics* **28,** 125–126 (2012).

Acknowledgements

The authors thank H. Pfanz for motivation to work on the studied mofettes, K. Henkel for assistance during thermogravimetric analysis, J. Wendt and H. Geilmann for assistance with TOC and δ^{13}C-TOC analysis, A. Hädrich, D. Akob, C. Simon, J. Kuhr and S. Vetter for help during sampling, and S. Kolb for discussions. Sequencing was performed by the Norwegian Sequencing Centre (www.sequencing.uio.no), a national technology platform supported by the Functional Genomics and Infrastructure programmes of the Research Council of Norway and the Southeastern Regional Health Authorities. This work was funded by the Deutsche Forschungsgemeinschaft through grant KU1367/10-1, the graduate research training group 'Alternation and element mobility at the microbe–mineral interface' (GRK 1257) and the German Centre for Integrative Biodiversity Research (iDiv) Halle-Jena-Leipzig.

Author contributions

F.B. conceived, designed and performed the experiments, analysed the data and wrote the main paper. T.U. helped to design and analyse metatranscriptome and -genome sequencing experiments. M.N. performed radiocarbon measurements of soil and plant material and helped with ^{13}C bulk soil measurements. S.E.T. and G.G. contributed to data discussion and structuring of the manuscript. G.D.G. and K.E.F. performed the metatranscriptome and -genome sequencing. F.B., K.K., S.E.T. and G.G. contributed to data discussion and structuring of the manuscript. All co-authors commented on and provided edits to the manuscript.

Additional information

Supplementary information is available online. Reprints and permissions information is available online at www.nature.com/reprints. Correspondence and requests for materials should be addressed to K.K.

Competing interests

The authors declare no competing financial interests.

Corrigendum: Altered carbon turnover processes and microbiomes in soils under long-term extremely high CO_2 exposure

Felix Beulig, Tim Urich, Martin Nowak, Susan E. Trumbore, Gerd Gleixner, Gregor D. Gilfillan, Kristine E. Fjelland and Kirsten Küsel

Nature Microbiology **1,** 15025 (2016); published online 27 January 2016; corrected 11 February 2016.

The version of this Article originally published listed an incorrect corresponding author. All versions of the Article have been amended to show that the corresponding author is Kirsten Küsel (kirsten.kuesel@uni-jena.de).